Available online at www.sciencedirect.com

SciVerse ScienceDirect

Energy Procedia 00 (2013) 000–000

Energy Procedia

www.elsevier.com/locate/procedia

SolarPACES 2013

Optical analysis and thermal modeling of a window for a small particle solar receiver

A. M. Mecit[a], F. J. Miller[a], A. Whitmore[a]

[a]*San Diego State University, Combustion and Solar Energy Laboratory, Mechanical Engineering, Room E327, San Diego 92182-1323, CA, USA*

Abstract

Concentrated solar power (CSP) systems use heliostats to concentrate solar radiation in order to produce high temperature heat, which drives a turbine to generate electricity. A 5 MW_{th} Small Particle Solar Receiver is being developed for power tower CSP plants based on volumetric absorption by a gas-particle suspension by the support from the U.S. Department of Energy under the SunShot Initiative. The radiation enters the pressurized receiver (0.5 MPa) through a curved window, which must sustain the thermal loads from the concentrated solar flux and infrared reradiation from inside the receiver. The thermal load from the solar flux on the window is calculated by using the computer code MIRVAL from Sandia National Laboratory which uses the Monte Carlo Ray Trace (MCRT) method, along with two other codes developed by the authors. Thermal loading was calculated from energy absorbed at various points throughout the window from both the heliostat field and inside the receiver. Transmission and reflective losses were also calculated for different window materials in order to find out how much radiation will enter the receiver or will be lost. The three dimensional temperature distribution of the window is analyzed by an energy balance taking into account spectral volumetric absorption, spectral surface emission, conduction within the window, and convection from both surfaces. A maximum window temperature of 800 ºC must be enforced to prevent cracking and/or devitrification due to overheating. Several grades of quartz are considered for this study with detailed spectral calculations. For a chosen material, the window temperature was found to be held under 800 ºC. The results showed that most of the heat load on the window comes from the inside of receiver due to spectral variation.

Selection and peer review by the scientific conference committee of SolarPACES 2013 under responsibility of PSE AG.

Keywords: Type your keywords here, separated by semicolons ; Fused Silica; Quartz; Window+; High Temperature; Monte Carlo Ray Trace; Solar; Solar Receiver; Thermal Analysis; Finite Volume; Internal Emission; High Temperature Radiation

*Corresponding author. Tel: +1 619-594-3599
E-mail address: fmiller@mail.sdsu.edu

Selection and peer review by the scientific conference committee of SolarPACES 2013 under responsibility of PSE AG.

1. Introduction

Concentrated solar power (CSP) systems use heliostats to concentrate the solar radiation. The concentrated solar radiation is used to heat a working fluid inside a receiver which drives a turbine to generate electricity. There are four types of CSP technologies: parabolic troughs, dish/engine systems, Linear Fresnel reflectors (LFRs), and power towers (1). Power towers use a field of heliostats to concentrate the solar radiation to the focal point of the heliostats at the top of the tower. The fluid flowing inside the receiver is heated by the concentrated radiation, with the details depending on the receiver design. The heat drives a thermodynamic cycle, always a Rankine cycle on commercial plants, to generate electricity. Compared to the LFRs and parabolic troughs, power towers can reach higher temperatures. The reason is that more solar radiation is concentrated on a smaller surface area which will reduce the heat losses. The thermodynamic cycles are more efficient when operating at higher temperatures. Therefore, higher efficiency can be achieved with power tower systems. These potential advantages make the power tower systems more appealing. These systems could soon become the preferred CSP technology (2). One of the challenges with central receivers, however, is the receiver design. Current commercial receivers cannot sustain the highest fluxes that a heliostat field is capable of producing, especially if using a gas as the working fluid, which is the desired working fluid for a gas turbine offering higher efficiency than the Rankine systems in use today. Therefore, we have re-initiated research on a previously researched concept for a gas-cooled receiver as described in the next section.

Nomenclature

r	radius	[m]
z	axial position	[m]
θ	angular position	[rad]
k	thermal conductivity	[W/(m-K)]
δ	grid cell length	[m]
λ	wavelength	[μm]
cp	specific heat	[J/kg-K]
T	temperature	[K]
S	source term	[W/m^3]
σ	Stefan-Boltzmann Constant	[$W/(m^2-K^4)$]
ε	Total Hemispherical Emissivity	[non-dimensional]
q''	Incoming Spectral Flux	[$W/(m^2-\mu m)$]

2. Small Particle Solar Receiver and other Receivers with Windows

The small particle solar receiver was first introduced by Hunt in the late 1970s (3). The small particle solar receiver is a large vessel with a window that allows the solar radiation into the receiver. Inside the receiver, a gas-particle suspension flows. This suspension contains air and smoke-like (sub-micron) carbon particles. The solar radiation is absorbed *volumetrically* by the carbon particles. As the carbon particles absorb the solar radiation, the temperature of the particles increases. Therefore, they heat the gas by conduction, which is very effective due to their small size. Eventually, the temperature increase of the suspension causes the carbon particles to oxidize. This process yields a hot, pressurized gas for use in Brayton cycle (3).

The Combustion and Solar Energy Laboratory at San Diego State University is currently working on modeling and designing a 5 MWth small particle solar receiver (4). The prototype will be built under the SunShot grant awarded by Department of Energy. The small particle solar receiver then will be tested at National Solar Thermal Test Facility (NSTTF). One key aspect of this receiver is the requirement for a large, pressurized window.

There are other several examples for windowed receivers. One of them is DLR receiver (5). The receiver is designed for solar-hybrid gas turbine and combined cycle systems and operates at 15 bar. It has a secondary concentrator at the inlet where the solar radiation enters the system right before the quartz window. A ceramic

absorber is put behind the window. The cold air enters the absorber and gets heated volumetrically through the absorber then exits the system. The exit temperature of the hot air is between 800 ˚C and 1000 ˚C.

Another example is the receiver tested at the Weizmann Institute in Israel (6). The receiver has a flat quartz window (type GE 124) and the transmission of the window was measured 87%. The radiation passing through the window is absorbed volumetrically in the receiver by the working fluid that is mixed with carbon particles. Due to thermal stability and high absorption in the entire solar spectrum, carbon particles were chosen to mix with the working fluid. Two working fluids were used: nitrogen and air. The energy flux of the concentrated solar radiation was up to 3 MW/m^2 and the size of carbon particles was around 3 μm in the experiments. The outlet temperature of the working fluid was in between 1343 K and 2118 K depending on the partial pressure ratio of the working fluid, the working fluid type, and the particle loading.

There have been several numerical simulations of small particle solar receivers. The first study, using a five-flux radiation model, was done by Miller in 1988, who modeled a lower temperature pipe flow system and compared it to lab-scale experiments (7). In 2010 a detailed radiation study was performed by Steven Ruther, using the Monte Carlo Ray Trace Method (MCRT) and an assumed slug flow fluid dynamics model (8). Later on, this model was improved by Crocker, by adding in a more realistic flow calculation (9). In these models the small particle receiver was limited to 2-D cylindrical and collimated uniform solar inputs. Both models had a fully transparent (no absorption and reflection) flat window. In reality the window will have both reflection and the absorption. It will be curved to withstand the pressure within the receiver. New models in 3-D was created by Fernandez del Campo for both a cylindrical and conical receiver (receiver with 45 degree wall angle), shown in Figure 1 (10). The new model is able to handle arbitrarily complex axisymmetric geometries. This allows the model to be coupled with a 3-D heliostat field and window model developed by Mecit (11). These latter models were used in this research to determine spectral intensity on the inside of the window.

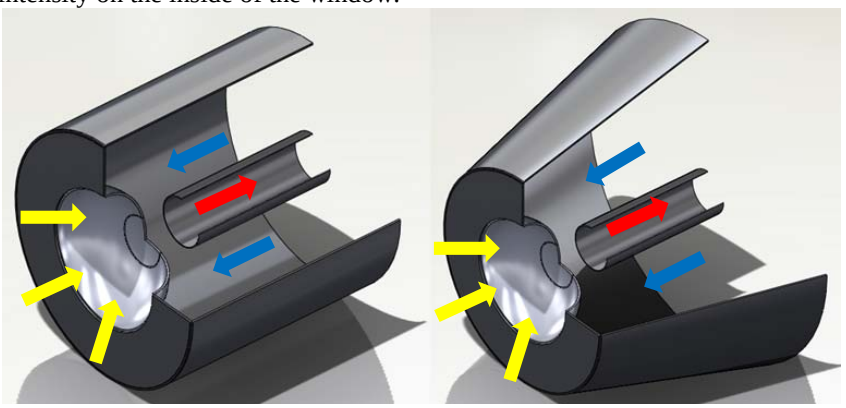

Figure 1 Schematic of the Two Models of the Small Particle Solar Receiver (yellow arrows: solar irradiation, blue arrows: air-particle mixture inlet, red arrows: air-particle mixture outlet). The cylindrical design on the left is referred to as design 1 and the conical design on the right is referred to as design 2 throughout this paper.

3. 3-D Heliostat Field and Window Model

The receiver model, mentioned above, needs to be supplied with an accurate solar irradiation input. MIRVAL is a computer code that we modified and use to compute the solar irradiation on a plane at the power tower, called the aperture plane, where the solar radiation is concentrated (12). MIRVAL also uses MCRT method which allows us easily couple it with receiver model. The details are explained by Mecit (11), (13).

A curved window is placed at the aperture plane to let the solar irradiation inside the receiver. The rays that are traced all the way from the sun to the aperture plane are then be traced until they meet the window. At the window, the fate of the rays is determined depending on the optical properties. The optical properties such as the absorptivity, the reflectivity, and the transmissivity of the window are a function of the wavelength and direction of the incoming radiation, and the index of refraction and the absorptive index of the material. A window model is developed to calculate the solar input arriving inside the receiver and the thermal load on the window (11), (13).

There are two main window shapes being studied so that the window will withstand the pressure within the receiver and help minimize the stresses caused by thermal and pressure loading as well as the amount of quartz needed. The first shape is a spherical window section. It was shown that this shape with a 60 degree cap angle minimizes the amount of the material needed in order to avoid buckling (14). The second shape is an ellipsoidal shape found by Onkar Mande (14), such that tensile stresses are eliminated and the entire window is under compression. In Mecit's research, the different cap angles varying from 0 to 90, in other words from flat to hemisphere, for a spherical window is studied as well as the ellipsoidal window (11), (13). Stress analysis for these spherical geometries is studied in Saung's paper (15). The diameter of the window is 1.7 m as picked in Mecit's research. In this paper, we will study a spherical cap window with a 45 degree cap angle. The reason is that the 45 degree spherical window is cheaper to manufacture compare to higher degree spherical windows and the ellipsoidal window and it will withstand the pressure from the receiver.

3.1. Evaluation of Different Window Materials

There are several window materials studied in Mecit's work (11), (13) . Some of these materials are as follows: Surprasil 3001/311, Suprasil 1/2 Grade A, HOQ 310, HSQ 300 etc. It is mentioned in these earlier papers that the absorptive index of the material for these materials given by the vendor are limited to certain wavelength range (0.946 μm to 1.319 μm). In this work, the information for the wavelength range up to at least 15 μm is needed to cover the rays both coming from the heliostat field as well as the rays emitted from inside the receiver.

Recently, more data for a wider wavelength range is obtained from the vendor. Data up to 5 μm for HOQ 310 is provided which covers the entire solar spectrum. Data up to 3 μm for Corning glass (code 7980, fused silica) is also provided. For calculation purposes and to cover entire solar spectrum (0.1μm up to 4μm), the data for HOQ 310 is used for the wavelength range of 3 to 5 μm (to fill in missing Corning data) as the aligned lines are seen in Figure 2. To display the absorbed energy per wavelength, 40 wavelength bands were picked with 0.1 μm intervals. The absorbed rays at the window were selected depending on the interval that they fall in. Then, the power of these rays was added up to find the absorbed energy per wavelength. For the study, ASTM G173 - 03(2012) Standard Tables for Reference Solar Spectral Irradiances: Direct Normal and Hemispherical on 37° Tilted Surface was used to simulate the wavelength distribution for the solar input (16). The study was done at 12 pm on March 21st for 2.5 cm thick spherical window (45 degree) with a radius of 0.85 m. The figure shows that the Corning glass has higher absorption compared to both Spectrosil 2000 and HOQ 310. The overall absorption for the HOQ 310 is 0.328%. The overall absorption for the corning glass is 0.865%. Expectedly, the overall absorption for the Spectrosil 2000 falls between these two materials and is 0.626%. According to the ASTM spectrum, only 1% of the rays coming from the sun have 3 μm or higher wavelength (16). Most of it is absorbed by the window (HOQ 310). The data for the Corning glass in this wavelength range should be obtained. In the wavelength range of 3 to 4 μm, Spectrosil 2000 behaves similarly compared to HOQ 310. Their absorption index values are very similar which leads to this similar behavior.

So far we have covered the optical properties of the window for the solar spectrum. A wider wavelength range should be studied since the rays coming from inside the receiver will have longer wavelengths. Earlier in Ruther's work, it was explained that that the upper wavelength cutoff can be chosen so that the excluded black body fraction is negligible. The approximate lower bound wall temperature of the small particle solar receiver is 1000 K. The chosen upper wavelength cutoff is 50 μm to exclude only 0.11 % of the black body fraction. This is a very small portion and is negligible (8). This value should be checked with the latest version of the receiver model which is created by Fernandez who also used the same cutoff. By using this model, we tracked the rays that are incident on the window from inside the receiver. In this study, a cylindrical receiver with 2 m radius and 3 m length is used with a 45 degree spherical cap window (HOQ 310) with a radius of 0.85 m, Figure 1. The study was done at 12 pm on March 21st with 26.5º tilt angle for the receiver. This study showed less than 1% of the rays have 15 μm or higher wavelengths. Figure 3 is plotted up to 15 μm for display purposes despite the calculation cutoff number of 50 μm. It shows the percentage of the rays with respect to their wavelength. In the calculations, 500 wavelength bands were used. The red line represents the rays (93.7% of the total rays) that are originated inside the receiver from the walls and the carbon particles). The oxidation of the carbon particles are not considered yet but the model is currently being modified for it. The peak of the red line (1.2 μm) is expected to shift to the right after that modification. The

blue line represents the rays (6.3% of the total rays) coming from the heliostats into the receiver and reflected back to the window due to scattering and wall reflection. The green line represents the total rays arriving from the receiver side.

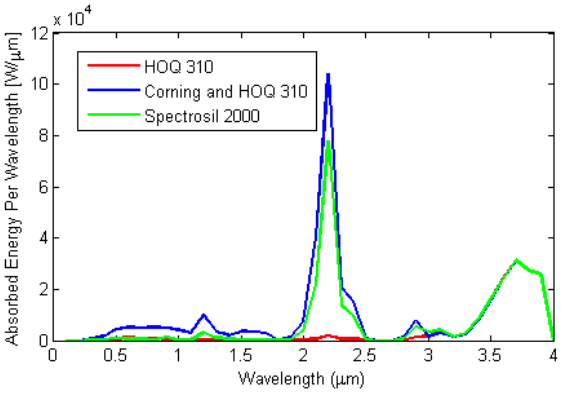

Figure 2 Absorbed Energy per Wavelength from the heliostat field.

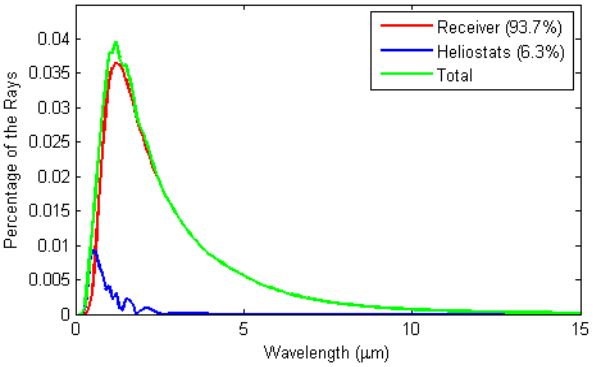

Figure 3 Wavelength Distribution of the Rays Reaching the Window from the Receiver Side

3.2. Absorbed Flux Maps on the Window

The absorbed flux on the window due to radiation is studied and shown in two different flux maps. One of the flux maps, Figure 4 (top view) and Figure 6 (isometric view), represents the absorbed radiation coming from inside the receiver and the other flux map, Figure 6 (note that the scale is different), shows the absorbed radiation coming from heliostat field. The figures have the same color bar limits. Result showed that the total absorption, or thermal load, at the window is 206.6 kW. Most of the thermal load, 92.7% (191.5 kW), is coming from inside the receiver. The reason is that the rays emitted from inside in the receiver have a longer wavelength as is it shown in Figure 3. In order to reduce the thermal load, the wall temperatures should be minimized by lowering the view factor. This can be done by changing the geometry of the receiver. A conical receiver (meaning angled walls) should be considered instead of a cylindrical receiver. With this approach, the rays will have a longer path length to get absorbed by the particles before reaching the walls. Fernandez has come up with different receiver geometry, the conical shape in Figure 1, explained in (17).

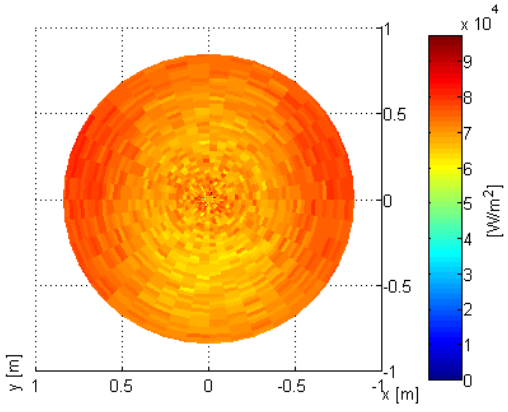

Figure 4 Top View (Looking from Inside the Receiver) of Absorbed Flux Map on the Window (Receiver Side, HOQ 310)

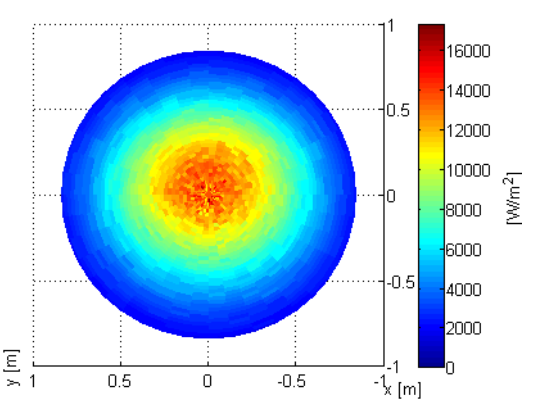

Figure 5 Top View (Looking from Inside the Receiver) of Absorbed Flux Map on the Window (Heliostat Side, HOQ 310)

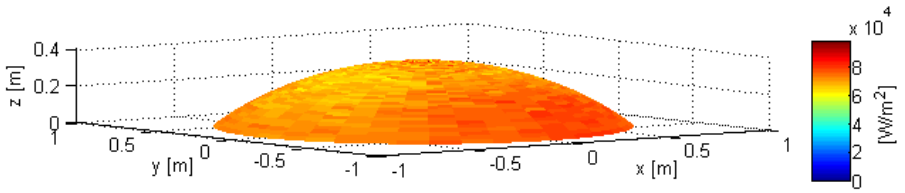

Figure 6 Absorbed Flux Map on the Window (Receiver Side, HOQ 310)

As seen in Figure 4, absorbed flux is higher around the right and left sides. The reason is that the receiver wall is hotter on two sides due to the heliostat field design. The heliostat filed has more heliostats to the right and left sides of the field looking from the receiver (11). Figure 5 shows the absorbed flux from the heliostat side. The flux from the heliostat side is lower compared to the receiver side due to infrared (IR) absorption.

3.3. Absorbed Power Depending on Receiver Design and the Window's Material Selection

Table 1 shows the importance of the conical shaped receiver design (Design 2) in reducing the power absorbed by the window. Table 1 also shows the importance of the material choice. Even though the total hemispherical emissivity is increased with the Spectrosil and Corning-HOQ-310 materials, their increased absorptivity dramatically outweighs the emissivity increase in our operating temperature ranges. The power absorbed is calculated for two different scenarios. The first is through Beer's law for normal collimated inputs, resulting in a total path length equal to the thickness of the window. The second is using the two flux method, which assumes isotropic flux with angle. This method increases the path length by a factor of two, increasing the total power absorbed (7). The best scenario is using the conical shaped receiver design (Design 2) with a window made of HOQ-310.

Table 1 Comparison of different window materials and receiver geometries

Scenario #	**1**	**2**	**3**	**4**	**5**	**6**	**7**	**8**	**9**	**10**	**11**	**12**
Material	HOQ-310	HOQ-310	Corning & HOQ-310	Corning & HOQ-310	Spectrosil	Spectrosil	HOQ-310	HOQ-310	Corning & HOQ-310	Corning & HOQ-310	Spectrosil	Spectrosil
Receiver Geometry Design	1	1	1	1	1	1	2	2	2	2	2	2
Total Receiver IR Absorbed (kW)	186	206	241	277	230	264	140	155	181	209	174	199
Total Solar Absorbed (kW)	14	22	37	62	27	44	14	22	37	62	27	44
Total Energy Absorbed (kW)	200	220	277	339	257	308	154	177	218	271	200	243
Receiver Radiation 2 Flux Model	No	Yes	No	Yes	No	Yes	No	Yes	No	Yes	No	Yes

4. 3-D Thermal Model of the Window to Determine the Temperature

The temperature of the window is determined by an energy balance between the solar energy absorbed, the energy absorbed from the receiver's thermal infrared radiation, the thermal radiation emitted from the window, the liquid cooled outer mounting ring, and convection on both sides of the window, refer to Figure 7. In cylindrical coordinates, a planar three dimensional finite volume code written in FORTRAN for this research is used to balance the energy and solve for the temperature distribution in the glass. A Beer's law source code written in FORTRAN for this research is used to determine where both the heliostat and receiver rays are absorbed within the window.

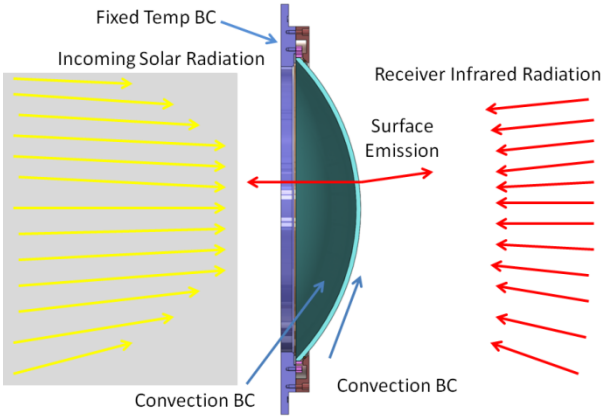

Figure 7 Boundary Conditions of the Energy Solver, Solar Rays come from the heliostat field at the NSTTF. Receiver rays are calculated from the 3-D receiver model. They include emitted radiation and radiation reflected back from inside the receiver (the latter not shown). See reference (10) for description of the receiver model.

4.1. Energy Solver Equations and Boundary Conditions

The energy solver is a steady state, planar*, three dimensional finite volume code written in 3-D cylindrical coordinates to solve the energy equation, Eqn (1). The code has spatially variable convection and fixed edge temperature boundary conditions. There are 40 radial control volumes, 40 angular control volumes and 20 axial control volumes; this has been validated as adequate by a grid convergence study. The radiation absorption is applied through the source term S. Beer's law is applied to determine how much power is absorbed spatially throughout the window, Eq (3,4). The surface emission is determined from the Stefan-Boltzmann law. The emissivity is calculated by using the index of refraction along with the absorptive index of the material as inputs into the Fresnel equations to calculate the angular, spectral reflectivity. Using Kirchhoff's law of thermal radiation, we get a spectral directional emissivity. Using Planck's law we integrate over all angles and wavelengths for each window temperature, to get a total hemispherical emissivity which is a function of temperature.

$$\rho C_P \frac{\partial T}{\partial t} = \frac{1}{r}\frac{\partial}{\partial r}\left(rk\frac{\partial T}{\partial r}\right) + \frac{1}{r}\frac{\partial}{\partial \theta}\left(\frac{k}{r}\frac{\partial T}{\partial \theta}\right) + \frac{1}{r}\frac{\partial}{\partial z}\left(k\frac{\partial T}{\partial z}\right) + S \tag{1}$$

$$S = S_{Solar\ Power\ Absorbed} + S_{Receiver\ Power\ Absorbed} - S_{Surface\ Emissions\ (Only\ From\ Surface\ Cells)} \tag{2}$$

$$S_{Solar\ Power\ Absorbed} = q''_{Solar} * \left(e^{\left(-\kappa_\lambda * \left(x+\frac{dx}{2}\right)\right)} - e^{\left(-\kappa_\lambda * \left(x-\frac{dx}{2}\right)\right)}\right) \tag{3}$$

$$S_{Receiver\ Power\ Absorbed} = q''_{Receiver} * \left(e^{\left(-\kappa_\lambda * \left(x+\frac{dx}{2}\right)\right)} - e^{\left(-\kappa_\lambda * \left(x-\frac{dx}{2}\right)\right)}\right) \tag{4}$$

$$S_{Surface\ Emissions} = Cell\ Surface\ Area * \varepsilon(T_{Local}, Material) * \sigma * T_{Local}^4 \tag{5}$$

* The energy solver model for the hemispherical cap window is modeled as planar because of the large radius of curvature. Locally the window is approximately flat.

The method described in (18) is used to solve the equation iteratively. The thermal conductivity k is taken constant at 1 W/m-K for this work, and while we have done transient heating cases, only steady state results are presented here meaning the first term is zero.

The receiver's internal emissions reaching the window are calculated using a three dimensional spectral MCRT/CFD code of the receiver created by Fernandez (10). The receiver's rays on the window are normal with local absorbed fluxes shown in Figure 5. The internal side of the window's local convection coefficients' and air temperatures are used as inputs to the window thermal analysis. These convection coefficients and film temperatures will be used in future CFD analyses to optimize the final receiver design. The exterior window surface is assumed to have forced convection with an ambient temperature of 333 Kelvin. The local convection coefficients on the exterior and interior surface are parameters which are used to keep the window's temperature gradients at a minimum while keeping the windows absolute temperatures below 1073 Kelvin. The mounting ring is assumed to be fixed at 300 Kelvin, representing active water cooling. Since the receiver is pressurized, there is a high temperature graphite sealing gasket, grafoil GTC. This gasket has a maximum temperature of 723 Kelvin. For this design we would like to keep the temperature of the gasket below 500 Kelvin, therefore active cooling of the mounting flange is needed.

The energy solver model has been verified against a grey, one dimensional analytical solution to the heat diffusion equation. A grid convergence was performed and the energy solver has a second order convergence rate. The energy solver has also been verified against Solidworks Simulation 2013, a three dimensional commercial available finite element program for the grey, constant source term case with varying boundary conditions. The MCRT codes were verified with ray convergence studies in Fernandez (10) and Mecit (11).

4.2. *Thermal Model Outputs*

Figure 8 is a slice through the center of the window which shows a typical result of a temperature field in the glass. The streaking in the horizontal direction is due to local variations in the receiver flux on the inside surface of the window. Note that the figure is stretched significantly in the axial direction to make the temperature field easier to see (the aspect ratio of the window is not 1:1 in the figure). The hottest spot is found to be near the inside surface of the glass due to the absorbed flux profile shown in Figure 5. The results shown in Figures 8, 9 and 10 are with interior convection coefficients of 30 W/(m^2-K) @ 600 Kelvin, exterior convection coefficients of 100 W/(m^2-K) @ 300 Kelvin, external edge temperature fixed to 300 Kelvin, and the two flux models used for absorption in the HOQ-310 window.

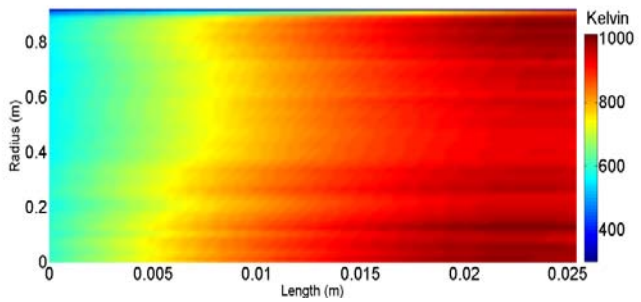

Figure 8 Window Temperature Profile (H0Q-310)

The maximum window temperature is 1070 Kelvin which is below our maximum temperature criterion of 1073 Kelvin meaning that Hereaus HOQ 310 is an adequate glass for this application. Figure 9 has a surface temperature view of the window as seen from inside.

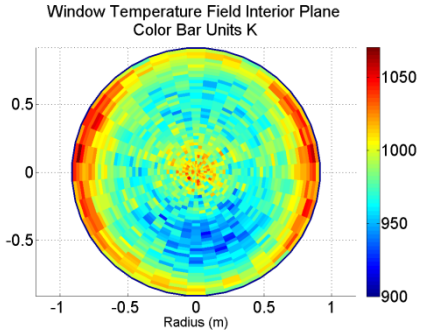

Figure 9 Window Temperature Field Interior Surface (Material is HOQ-310)

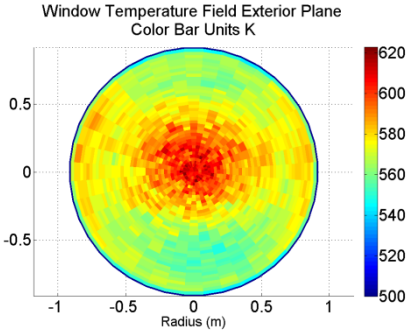

Figure 10 Window Temperature Field Exterior Surface (Material is HOQ-310)

Finally, Figure 11 shows the absolute temperature gradient field in the glass. These interesting results show that the inside of the window has the highest temperature gradients, which is to be expected because of the large absorbed flux shown in Figure 4. Also by increasing the fixed edge temperature, the maximum temperature gradient can be reduced while minimally affecting the maximum temperature of the window. Work by Saung is quantifying the maximum temperature gradient that can be tolerated (19).

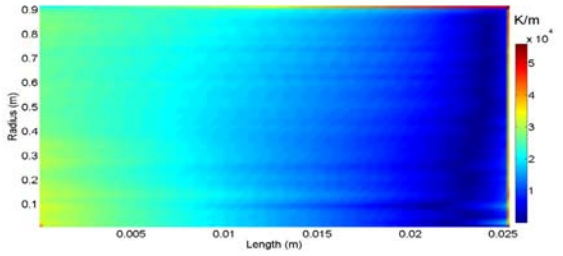

Figure 11 Window Temperature Gradient Field, (HOQ-310)

4.3. *Thermal Model Parameter Study*

Table 2 The Effects of Interior and Exterior convection coefficient as well as the Temperature

Scenario #	1	2	3	4	5	6	7	8
h_interior (W/m^2K)	10	20	30	30	30	50	100	30
h_exterior (W/m^2K)	100	100	100	50	10	10	100	100
T_int (K)	500	700	600	500	500	500	700	600
T_ext (K)	333	333	333	333	333	333	333	333
Fixed Edge Temperature (K)	300	300	300	300	300	300	300	600
Power Conv Int (kW)	-73	-16	-28	-37	-40	-58	-49	-29
Power Conv Ext (kW)	-48	-65	-63	-44	-13	-12	-58	-64
Power Conducted Edge (kW)	-39	-5	-5	-5	-6	-5	-5	-2
Power Emitted Int (kW)	-42	-113	-96	-92	-95	-75	-70	-97
Power Emitted Ext (kW)	-1	-9	-9	-16	-34	-32	-8	-9
Max Window Temperature (K)	883	1114	1070	1082	1130	1073	980	1073

Table 2 demonstrates the importance of the interior and exterior convection coefficients and temperatures in relation to the maximum window temperature. The maximum window temperature is highlighted in green and red to indicate if it is below the maximum window temperature criterion of 1073 Kelvin, passing and failing respectively.

5. Conclusions

In conclusion, HOQ 310 is viable material for a pressurized solar receiver window. HOQ 310 has a high enough maximum temperature and low enough absorption to withstand the high infrared and solar radiation fluxes. Forced convection cooling of the window is needed to keep the maximum temperature below 1073K. This analysis has ruled out Spectrasil and Corning as possible material choices because of their large absorption. A minimum interior side convection coefficient of 10 W/(m^2-K) with a film temperature of 500K. There is future work in designing the forced convection cooling method and calculating the required convection coefficients. Also a Monte Carlo Ray Code will be used to calculate the absorption of both the receiver rays and the solar rays within the window, while also calculating the internal emission within the window (not just surface emission). The numerical models which have been developed for this work can now be easily adapted to other engineering problem related to high temperature glass problems and pressurized solar receivers.

Acknowledgements

The authors gratefully acknowledge the U.S. Department of Energy for providing funding for this research through the SunShot Initiative under the Award #DE-EE0005800. We would also like to thank Aerojet Rocketdyne, Solar Turbines and Thermaphase Energy for their support to the project.

References

[1] Gerrefi, G. And Dubay, K., "Concentrating Solar Power Clean Energy for the Electric Grid", Boston: Mc-Graw-Hill/Irwin, 2008.

[2] International Renewable Energy Agency, "Renewable energy Technologies: Cost Analysis Series", Vol. 1, Power Sector 2/5, June 2012.

[3] Hunt, A. J., "A New Solar Thermal Receiver Utilizing Small Particles", Atlanta, GA: Proc. Int. Solar Energy Society Conf., 1979,pp. 1326-1366.

[4] Miller, F. J. and Hunt, A. J., "Developing the Small Particle Heat Exchange Receiver for a Prototype test", ASME 2012 6th International Conference on Energy Sustainability, San Diego, CA, 2012.

[5] Heller, P., Pfander, M., Denk,T., Tellez, F., Valverde, A., Fernandez, J. and Ring, A.,"Test and Evaluation of a Solar Powered Gas Turbine System", Solar Energy, Vol., 80, pp. 1225-1230, 2006.

[6] Helena, K. H., Rubin, R. and Karni, J., "Experimental Evaluation of Particle Consumption in a Particle Seeded Receiver", SolarPACES International Symposium, Spain, June 2006.

[7] Miller, F., "An Experimental and Theoretical Study of Heat Transfer in a Gas-Particle Flow Under Direct Radiant Heating", Department of Mechanical Engineering, University of Berkeley, Berkeley, CA, 1988.

[8] Ruther, S. J., "Radiation Heat Transfer Simulation of a Small Particle Solar Receiver Using the Monte Carlo Ray Trace Method", Master's Thesis, Department of Mechanical Engineering, San Diego State University, San Diego, CA, 2010.

[9] Crocker, A. W., "Coupled Fluid Flow and Radiation Modelling of a Small Particle Solar Receiver", Master's Thesis, Department of Mechanical Engineering, San Diego State University, San Diego, CA, 2012.

[10] Fernandez, P., Crocker, A. W. and Miller. F. J., "Three-Dimensional Fluid Dynamics and Radiative Heat transfer Modelling of a Small Particle Solar Receiver", ASME, 7th Conference on Energy Sustainability & 11th Fuel Cell Science, Engineering and Technology Conference, ES-FuelCell-2013-18149, Minneapolis, MN, 2013.

[11] Mecit, A. M., "Optical Analysis and Modelling of a Window for the Small Particle Receiver Using the Monte Carlo Ray Trace Method", Master's Thesis, Department of Mechanical Engineering, San Diego State University, San Diego, CA, 2013.

[12] Leary, P. L. and Hankins, J. D., "A User's Guide for MIRVAL-A Computer Code for Comparing Design of Heliostat-Receiver Optics for Central Receiver Solar Power Plants", Sandia National Laboratory, SAND77-8280, February 1979.

[13] Mecit, A. M., "Optical Analysis of a Window for Solar Receivers Using the Monte Carlo Ray Trace Method", ASME, 7th Conference on Energy Sustainability & 11th Fuel Cell Science, Engineering and Technology Conference, ES-FuelCell-2013-18186, Minneapolis, MN, 2013.

[14] Mande, O. K., "Window Seal Design for a Small Particle Solar Receiver", Master's Thesis, Department of Mechanical Engineering, San Diego State University, San Diego, CA, 2011.

[15] Saung, E. and Miller, F. J. "Dome Window Geometry for a Large Scale Solar Receiver", ASME, 7th Conference on Energy Sustainability & 11th Fuel Cell Science, Engineering and Technology Conference, ES-FuelCell-2013-18217, Minneapolis, MN, 2013

[16] http://www.astm.org/Standards/G173.htm., ASTM G173-03(2012) Standard Tables for Reference Solar Spectral Irradiances: Direct Normal And Hemispherical on 37º Tilted Surface. [Online]

[17] Fernandez, P., Miller, F., McDowell, Hunt, A.,"Design Space Exploration of a 5 MW_{th} Small Particle Solar Receiver", SolarPACES International Symposium, Las Vegas, NV, USA, September 17-20, 2013.

[18] Pantakar. "Numerical Heat Transfer and Fluid Flow", Hemisphere Publishing Corporation, 1980.

[19] Saung, E. and Miller, F. J., "Dome Window Mount Design for a 5 MW_{th} Solar Receiver", SolarPACES International Symposium, Las Vegas, NV, USA, September 17-20, 2013.